Supporting Information

Takayama and Clore 10.1073/pnas.1100050108

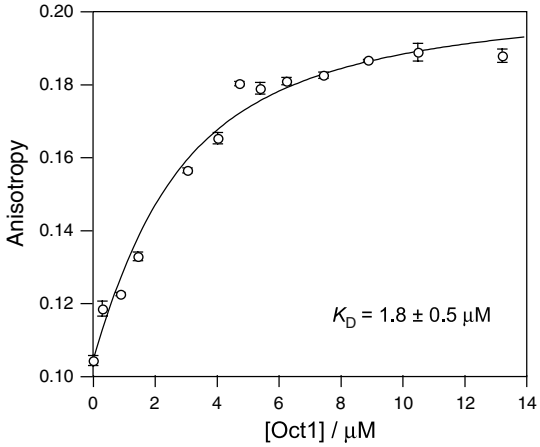

Fig. S1. Nonspecific binding of Oct1 to DNA monitored by fluorescence anisotropy. The sequence of the nonspecific 24-bp DNA duplex is shown in Fig. 1*A* of the main text, and the rhodamine fluorescent label is conjugated to the 5′ end of the bottom strand. The concentration of DNA is 1.7 μM in 10 mM Tris-HCl pH 7.4 and 150 mM NaCl. The excitation and emission wavelengths are 550 and 580 nm, respectively. The experimental data points (error bars, 1 SD) are shown as filled-in circles, and the best-fit curve with an apparent K_D of 1.8–0.5 μM is shown as a solid line.

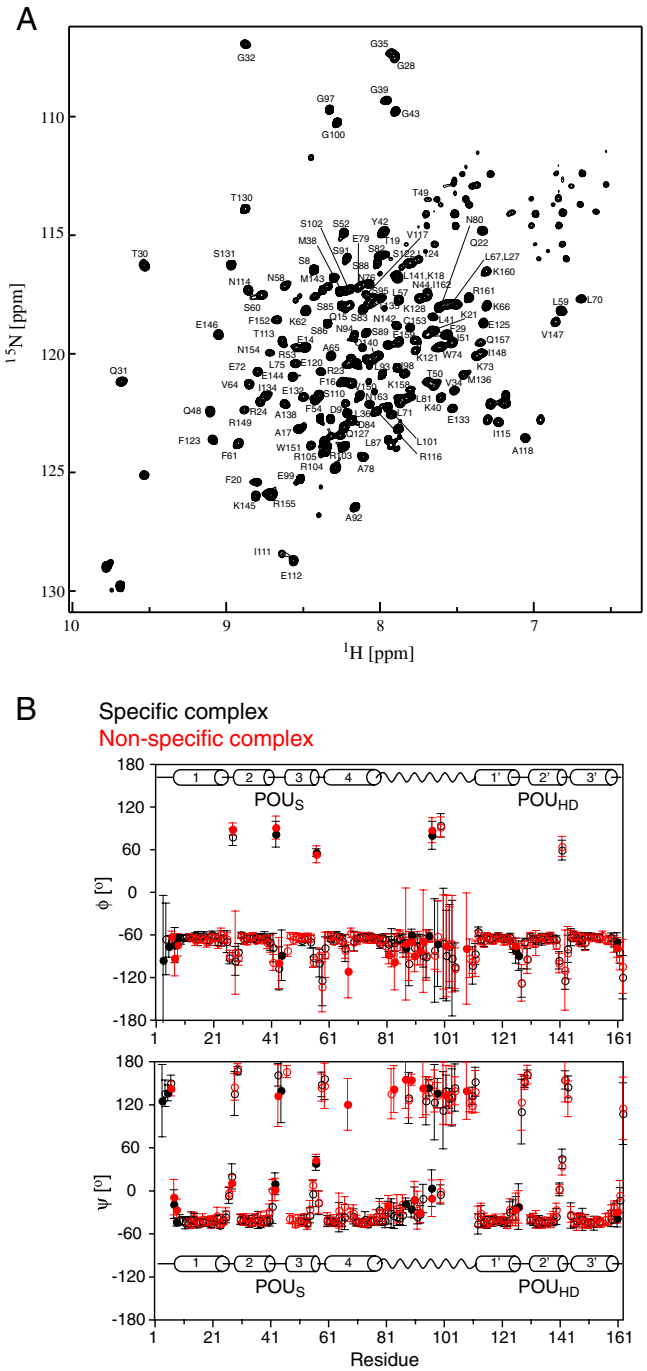

Fig. S2. (*A*) Assignment of the ^{1}H-^{15}N TROSY correlation spectrum of the nonspecific Oct1-DNA complex. The sequence of the nonspecific 24mer DNA duplex is shown in Fig. 1*A* of the main text. (*B*) ϕ/ψ backbone torsion angles for the specific (black) and nonspecific (red) Oct1-DNA complexes derived from backbone $^{1}H_N/^{13}C\alpha/^{13}C\beta/^{13}C'/^{15}N$ chemical shifts using the program TALOS+ (1). Residues whose ϕ/ψ predicted dihedral angles are uncertain are shown as filled-in circles. (Error bars, 1 SD)

1 Shen T, Delaglio F, Cornilescu G, Bax A (2009) TALOS+: a hybrid method for predicting protein backbone torsion angles from NMR chemical shifts. *J Biomol NMR* 44:213–223.

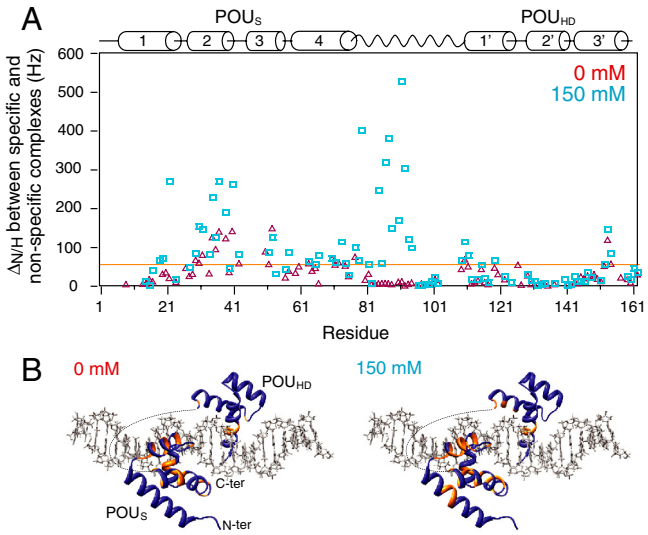

Fig. S3. (*A*) Backbone $^{1}H_{N}/^{15}N$ chemical shift difference profile between the specific and nonspecific complexes at 0 (purple) and 150 (cyan) mM NaCl ($\Delta_{N/H} = [(\Delta\delta_H)^2 + (\Delta\delta_N)^2]^{1/2}$ in Hz at a ^{1}H frequency of 500 MHz). (*B*) Residues showing large ($\Delta_{N/H}$ > 50 Hz; above the orange line) perturbations are mapped in orange on the tertiary structure of the specific Oct1-DNA complex.

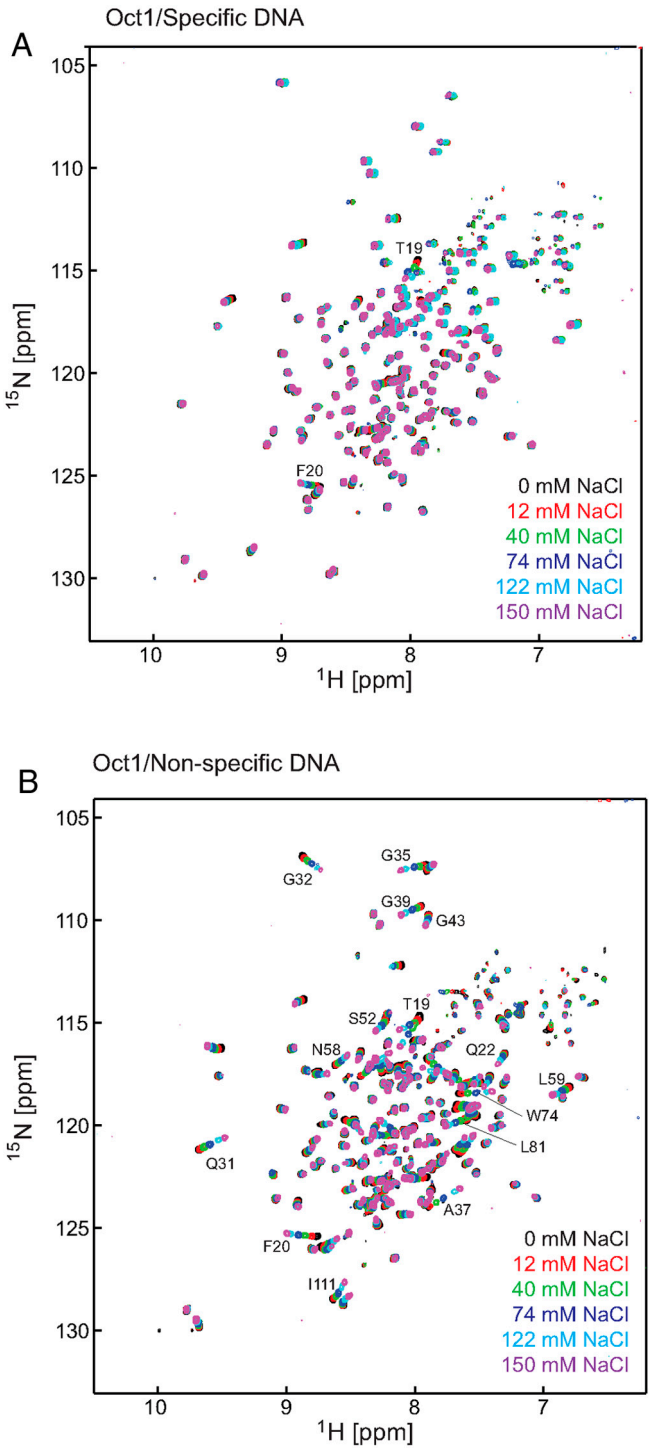

Fig. S4. Effect of salt-titration on the ^{1}H-^{15}N TROSY correlation spectra of the (*A*) specific and (*B*) nonspecific Oct1-DNA complexes. Concentrations of NaCl are 0 (black), 12 (red), 40 (green), 74 (blue), 122 (cyan), and 150 (purple) mM. The concentrations of Oct1 and 24-bp DNA duplexes are 0.2 and 0.3 mM, respectively.

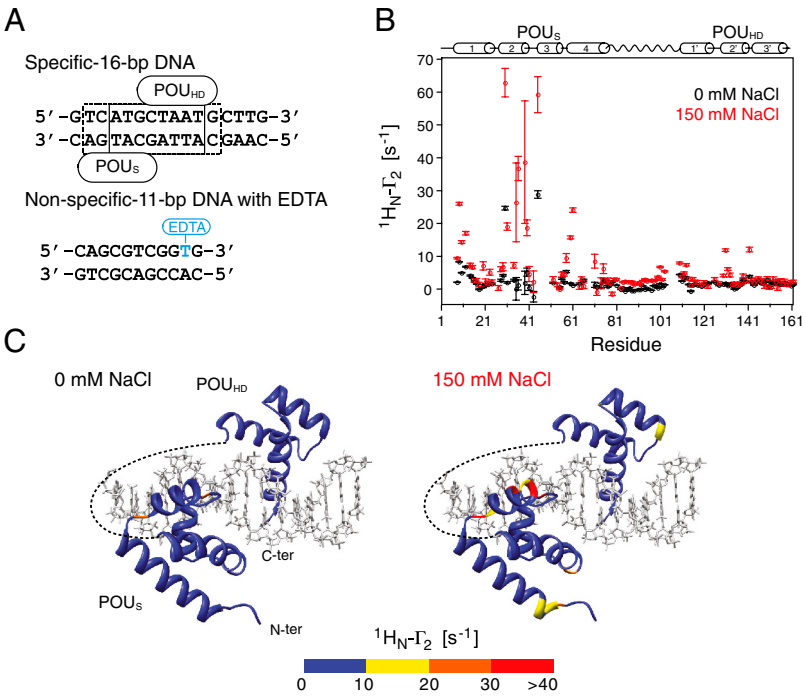

Fig. S5. Demonstration of intermolecular translocation by PRE. (*A*) The sample comprises an equimixture of an unlabeled 16-bp DNA duplex containing the specific target site of Oct1 and a paramagnetically (dT-EDTA-Mn^{2+}) labeled 11-bp nonspecific DNA duplex. In this sample, intermolecular PREs on Oct1 bound specifically to DNA can only be observed as a consequence of transient intermolecular translocation from the specific DNA duplex to the nonspecific DNA duplex and back again. (*B*) Intermolecular PRE profiles for Oct1 at 0 (black) and 150 (red) mM NaCl. The concentrations of Oct1, 16-bp specific DNA, and 11-bp nonspecific DNA are 0.40, 0.44, and 0.44 mM, respectively. (*C*) PRE profiles at 0 (left) and 150 (right) mM NaCl mapped onto the structure of the specific Oct1-DNA complex. The Γ_2 color scale is shown below the figure. PREs are predominantly observed for the POU_S domain, although a few small PREs are observed at high salt in helix 2′ of the POU_{HD} domain, indicating that the POU_S domain undergoes substantial intermolecular translocation.